



SiliconPV: March 25-27, 2013, Hamelin, Germany

High Resolution Inline Topography of Iron in P-doped Multicrystalline Bricks by MDP

Nadine Schüler^{a,*}, Bastian Berger^a, Adrienne Blum^b, Kay Dornich^a, Jürgen R. Niklas^a

^aFreiberg Instruments, Delfter Str. 06, 09599 Freiberg, Germany

^bSinton Instruments, 4720 Walnut Street, Suite 102, Boulder, CO 80301, USA

Abstract

The iron density is one crucial parameter to verify the quality of the material. Brick measurements enable to check the material quality right at the beginning of the production line. This paper presents contact less high resolution inline topographic measurements of the iron density in multicrystalline silicon bricks by MDP (microwave detected photoconductivity). The measurement procedure is fully automatic and takes less than 5 min a brick. The data obtained were compared to QSSPC (quasi steady state photoconductivity) measurements, however, with a loss in spatial resolution. Furthermore, passivated wafers were prepared from the bricks after the measurements and investigated individually. The consistency of all the data is remarkable.

© 2013 The Authors. Published by Elsevier Ltd.

Selection and/or peer-review under responsibility of the scientific committee of the SiliconPV 2013 conference

Keywords: Lifetime; iron; multicrystalline silicon; brick; MDP

1. Introduction

Contact less measurements of the minority carrier lifetime are a widely spread method to determine the material quality especially in the PV industry. The minority carrier lifetime is very sensitive to structural defects as well as impurities as the here investigated iron. Hence the lifetime is an ideal parameter to classify wafers and even bricks. Commonly used methods are μ PCD (microwave detected photoconductivity decay) [1], QSSPC (quasi steady state photo conductance) [2] and the method MDP [3] applied here. Another widely used method is the photoluminescence method (PL), where instead of measuring the photoconductivity as in the methods mentioned before, the photoluminescence intensity is

* Corresponding author. Tel.: +49-3731-4195419; fax: +49-3731-4195414.
E-mail address: schueler@freiberginstruments.com.

measured [4]. For the PL measurements usually a calibration for quantitative lifetime values is needed. Considering lifetime measurements on bricks, all four methods differ with respect to their penetration depth, measurement speed and spatial resolution.

In former papers the method MDP was already introduced to the field of inline measurements on wafers and bricks and its speed and high resolution were demonstrated [5]. It was shown that the penetration depth at bricks is much higher (≈ 1 mm) than for μ PCD (< 200 μ m) [6]. QSSPC exhibits even ≈ 2.5 mm penetration depth, however, with a spatial resolution unsatisfactory for topograms. The reason for these different penetration depths is mainly due to the measurement regime and the developing carrier profile in the sample. In a steady state or quasi-steady state regime the carriers can diffuse into the depth of the sample and the surface has a smaller impact on the measurements [6,7]. Hence MDP and QSSPC provide bulk dominated data whereas μ PCD is dominated by surface recombination. Nonetheless there is still an influence of the surface recombination on MDP measurements and hence the measured lifetimes are slightly smaller than the ones measured by QSSPC. However, for the accuracy of the iron detection it is only necessary to gain a lifetime difference between the two states (FeB and Fe_i) and that the surface recombination is not changed during the dissociation, which is not the case. To determine the iron content in a p-doped silicon sample, the lifetime before, τ_{FeB} and after the dissociation of FeB pairs, τ_{Fe_i} is used. Since Fe_i and FeB are different recombination centers with different properties, a change in the measured lifetime can be detected upon the dissociation of FeB pairs. The iron content can then be determined by using the following equation [8]:

$$[Fe] = C(\Delta n, N_{dot}) \cdot \left(\frac{1}{\tau_{Fe_i}} - \frac{1}{\tau_{FeB}} \right) \quad (1)$$

As stated above one premise is that the lifetime effect is not masked by other dominant recombination paths such as the surface. Hence an iron determination on wafers is only possible, if they are passivated. For bricks, in contrast, MDP and QSSPC enable iron determinations with *unpassivated* surfaces. Also PL measurements enable the iron detection in bricks, but again a calibration is needed. However, so far the accuracy of iron content measurements in bricks is still an issue. One problem is the determination of the injection level, since in bricks no uniform carrier profile is present during the measurement. The injection level is necessary to determine the calibration factor C (equ.1) for the iron determination.

The accuracy of the results was checked by correlations between MDP and QSSPC data and by measurements on SiN_x - passivated wafers as prepared from the bricks.

2. Experimental

The time dependent photoconductivity during and after a rectangular light pulse was measured by an advanced microwave detections system (MDP). Measurements under a steady state photo generation regime (pulse width: 200 μ s, laser power: 500 mW, spot diameter: 500 μ m) were used to achieve a high penetration depth of the generated carriers and an injection that is well above the crossover point of FEB and Fe_i. The lifetime is determined from the time constant of the decay after the light is switched off (more details can be found in [6]). For the MDP brick measurements the MDPingot inline equipment (Freiberg Instruments) was used. Measurement time is less than 20 s for a standard map and 1 min for an iron topogram, respectively. For the iron measurements, a map before and again after the irradiation of the sample by flash lights was used. The flash light (Mono Max 1500 by Hensel with 1500 J) is integrated into the measurement system and the samples is flashed 20 times for 1 ms. Since the doping density in mc-Si is around $10^{15} \dots 10^{16}$ cm⁻³ all electrically active Fe is present as FeB pairs before the irradiation.

The samples are irradiated according to [9] and so that it is ensured that the FeB and Fe_i states are formed completely before and after the irradiation.

First an iron measurement of one face of a brick was performed by MDP and QSSPC (Sinton Instruments). The brick investigated was prepared from the edge of an ingot. Afterwards the brick was cut into wafers, which were passivated with SiN_x. Iron measurements were performed on the wafers and correlated to the results obtained for the brick. The following measurement conditions were used.

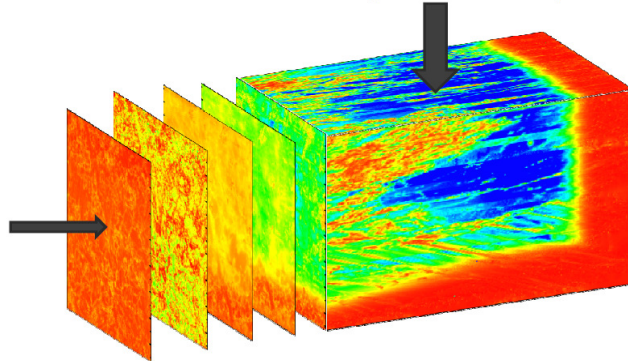


Fig. 1. Scheme of the measurement of one face of the brick and the passivated wafers

Table 1. Measurement conditions

Parameter	MDP	QSSPC
excited area [mm]	0.8 (spot)	3 x 40 (area)
pulse width [μs]	200	
resolution/step width [mm]	1 (full map)	3 (stripe)
frequency [Hz]	9.4 x 10 ⁻⁹	10 ⁷
light wavelength [nm]	978	> 810
injection [cm ⁻³]	10 ¹⁵ ...10 ¹⁶	10 ¹⁵

3. Determination of injection level and calibration factor

As explained above, in bricks a non uniform carrier density profile is present. Hence only a weighted average of the injection can be determined.

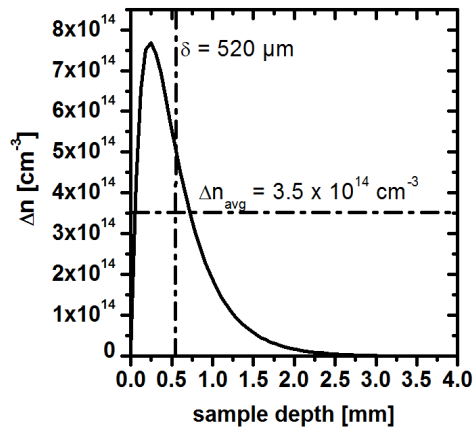


Fig. 2. typical carrier profile with marked skin depth δ and weighted average injection level for a resistivity of 1 Ωcm

For MDP measurements the light penetration depth was modeled and from that the carrier density profile was determined. This profile was convoluted with the skin depth of the applied microwave and the weighted average was determined as follows [10]:

$$\Delta n_{avg} = \frac{\int_0^w \Delta n(x)w(x)dx}{\int_0^w w(x)dx} \tag{2}$$

with the weighing function $w(x) = e^{-\frac{x}{\delta}}$ (3)

and skin depth $\delta = \sqrt{\frac{\rho}{\pi\mu_0\mu_r\nu}}$ (4)

whereas ν is the frequency of the applied microwave (for MDP $\nu = 9.4$ GHz).

For QSSPC measurements a similar approach was used, where the modeled profile was convoluted with the sensitivity depth of the sensor [11]. In previous publications often the approach from Bowden et al. [12] was used, where the modeled profile was convoluted with itself, but measurements and simulations suggest that it is more accurate to use the skin depth or sensor depth.

The accuracy of the iron determination is strongly dependent on the correct calibration factor C (equ. 1). In this study the calibration factor was determined according to the model of Macdonald et al. [13]. Since MDP measurements are performed at the same generation rate (laser power) rather than the same injection level, the calibration factor has to be determined according to the following equations [14]:

$$C = \frac{1}{\chi_{FeB} - \chi_{Fe_i}} \tag{5}$$

with

$$\chi_{FeB} = \frac{\nu_{th} \sigma_n^{FeB} (N_A + \Delta n_{FeB})}{(N_A + p_1^{FeB} + \Delta n_{FeB}) + k(n_1^{FeB} + \Delta n_{FeB})} \tag{6}$$

$$\chi_{Fe_i} = \frac{\nu_{th} \sigma_n^{Fe_i} (N_A + \Delta n_{Fe_i})}{(N_A + p_1^{Fe_i} + \Delta n_{Fe_i}) + k(n_1^{Fe_i} + \Delta n_{Fe_i})} \tag{7}$$

These equations are only valid, if no influence of traps or Auger recombination is present. Since the MDP measurements were performed with an injection level between 10^{15} and 10^{16} cm^{-3} these requirements are met.

4. Results

Figure 3(a) shows the measured iron density map of a brick and figure 3(b) a typical iron density map of one of the wafers. As expected, the edge face exhibits a much higher iron density than the rest of the brick, which causes an increased iron density at the lower edge of the wafer. However, this higher iron density cannot be detected by this brick measurement due to the maximum measurement sensitivity depth of 2.5 mm. Hence only a 1 mm stripe on the wafers adjacent to the measured brick face was correlated to the brick measurement.

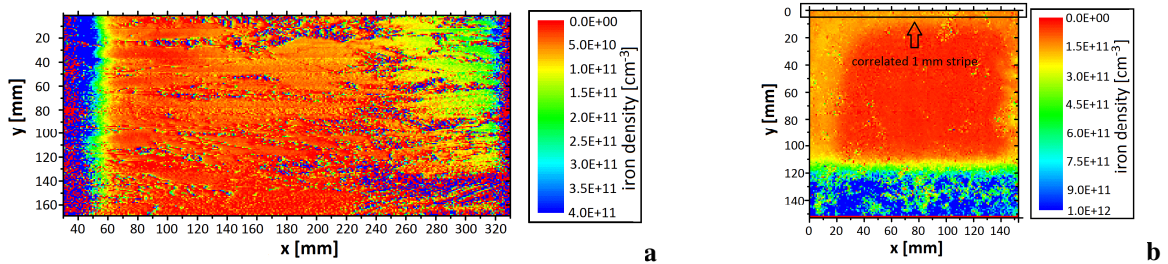


Fig. 3. (a) MDP Iron density map of the brick and (b) of an exemplary passivated wafer out of this brick

The results are shown in figure 4. The correlation between the different methods is very good. Small deviations are expected due to the different spatial averaging inherent in the MDP and QSSPC method. The deviations from the wafer measurements are in the order of the statistical errors of the wafer measurements. Considering the fact that with QSSPC and MDP very different experimental approaches are involved, the general data consistency obtained is remarkable. Apparently, also all the uncertainties inherent with the determination of the injection level do not play too big a role. In particular, the somewhat lower measurement sensitivity penetration depth of MDP compared to QSSPC has no significant effect. This all together provides a good piece of confidence considering the accuracy of the iron data as obtained by MDP maps.

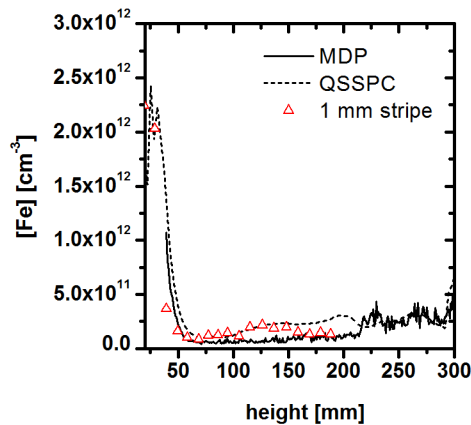


Fig. 4. Iron density versus brick height by MDP and QSSPC, and MDP wafer measurements (red triangles).

5. Conclusion

In this paper the applicability and accuracy of the MDP inline approach for automated topographic measurements of the iron density of bricks were investigated. As it is obvious from the results, the combination of measurement speed, spatial resolution, and reliability of the data as obtained by inline MDP is so far unparalleled.

References

- [1] Lauer, K., Laades, A., Übensee, H., Metzner, H., Lawerenz, A., Detailed analysis of the microwave-detected photoconductance decay in crystalline silicon. *Journal of Applied Physics* 2008 **104**, 104503.
- [2] Sinton, R.A., Cuevas, A., Contactless Determination of Current-Voltage Characteristics and Minority-carrier Lifetimes in Semiconductors from Quasi-steady-state Photoconductance Data, *Appl. Phys. Lett.* 1996, **69**, 2510–2512
- [3] Berger, B., Schüler, N., Anger, S., Gründig-Wendrock, B., Niklas, J. R., Contactless electrical defect characterization in semiconductors by microwave detected photo induced current transient spectroscopy (MDPICTS) and microwave detected photoconductivity (MDP). *phys. stat. sol. (a)* 2011, **208**, 769–776
- [4] Mitchell, B., Trupke, T., Weber, J. W., Nyhus, J., Bulk minority carrier lifetimes and doping of silicon bricks from photoluminescence intensity ratios, *Journal of Applied Physics* 2011, **109**, 1-12
- [5] Dornich, K., Schüler, N., Mittelstrass, D., Krause, A., Gründig-Wendrock, B., Niemietz, K., Niklas, J. R., New Spatial resolved inline metrology on multicrystalline silicon for PV, *Proceedings of the 24th PVSEC*, Hamburg, Germany, 2009, 1106-1009
- [6] Schueler, N., Dornich, K., Niklas, J.R., Gruendig-Wendrock, B., Theoretical and experimental comparison of contact less lifetime measurement methods at thick silicon samples, *Solar Energy Materials and Solar Cells* 2010 **94**, 1076-1082
- [7] Sinton, R., Trupke, T., Limitations on the dynamic excess carrier lifetime calibration methods, *Progress in Photovoltaics: Research and Applications* 2011, 1-4
- [8] Zoth, G., Bergholz, W., A fast, preparation-free method to detect iron in silicon. *Journal of Applied Physics* 1990. **67**, 6764–6771.
- [9] Macdonald, D. H., Geerligs, L. J., Azzizi, A., Iron detection in crystalline silicon by carrier lifetime measurements for arbitrary injection and doping, *Journal of Applied Physics* 2004, **98**, 1021-1028
- [10] Hahn, T., Numerische Modellierung und quantitative Analyse der Mikrowellendetektierten Photoleitfähigkeit (MDP) (Thesis) 2008.
- [11] Swirhun, J.S., Sinton, R.A., Forsyth, M.K., Mankad, T., Contactless measurement of minority carrier lifetime in silicon ingots and bricks. *Progress in Photovoltaics: Research and Applications* 2010.
- [12] Bowden, S., Sinton, R., Determining lifetime in silicon blocks and wafers with accurate expressions for carrier density, *Journal of Applied Physics* 2007, **102**, 124501
- [13] Macdonald, D., Roth, T., Deenapanray, P.N.K., Trupke, T., Bardos, R.A., Doping dependence of the carrier lifetime crossover point upon dissociation of iron-boron pairs in crystalline silicon. *Applied Physics Letters* 2006, **89**, 142107.
- [14] Macdonald, D., Tan, J. & Trupke, T. Imaging interstitial iron concentrations in boron-doped crystalline silicon using photoluminescence. *Journal of Applied Physics* 2008, **103**, 073710–1 – 073710–7